

Effect of self–interaction on the phase diagram of a Gibbs–like measure derived by a reversible Probabilistic Cellular Automata

Emilio N.M. Cirillo

E-mail: emilio.cirillo@uniroma1.it

Dipartimento di Scienze di Base e Applicate per l'Ingegneria, Sapienza Università di Roma, via A. Scarpa 16, I-00161, Roma, Italy.

Pierre–Yves Louis

E-mail: pierre-yves.louis@math.univ-poitiers.fr

Laboratoire de Mathématiques et Applications, UMR 7348 Université de Poitiers & CNRS, Téléport 2 - BP 30179 Boulevard Marie et Pierre Curie, F-86962 Technopole du Futuroscope de Poitiers Cedex, France

Wioletta M. Ruszel

E-mail: W.M.Ruszel@tudelft.nl

Delft Institute of Applied Sciences, Technical University Delft, Mekelweg 4, 2628 CD Delft, The Netherlands

Cristian Spitoni

E-mail: C.Spitoni@uu.nl

Institute of Mathematics, University of Utrecht, Budapestlaan 6, 3584 CD Utrecht, The Netherlands

Abstract. Cellular Automata are discrete–time dynamical systems on a spatially extended discrete space which provide paradigmatic examples of nonlinear phenomena. Their stochastic generalizations, i.e., Probabilistic Cellular Automata (PCA), are discrete time Markov chains on lattice with finite single–cell states whose distinguishing feature is the *parallel* character of the updating rule. We study the ground states of the Hamiltonian and the low–temperature phase diagram of the related Gibbs measure naturally associated with a class of reversible PCA, called the *cross PCA*. In such a model the updating rule of a cell depends indeed only on the status of the five cells forming a cross centered at the original cell itself. In particular, it depends on the value of the center spin (*self–interaction*). The goal of the paper is that of investigating the role played by the self–interaction parameter in connection with the ground states of the Hamiltonian and the low–temperature phase diagram of the Gibbs measure associated with this particular PCA.

Pacs: 05.45.-a; 05.50.+q; 64.60.De

Keywords: Probabilistic Cellular Automata, Phase Diagram, Mean Field Approximation

1. Introduction

Cellular Automata (CA) are discrete-time dynamical systems on a spatially extended discrete space. They are well known for – at the same time – being easy to define and implement and for exhibiting a rich and complex nonlinear behavior as emphasized for instance in [37,38] for CA on one-dimensional lattice. See [22] to precise the connections with the nonlinear physics. For the general theory of deterministic CA we refer to the recent paper [20] and references therein.

Probabilistic Cellular Automata (PCA) are CA straightforward generalization where the updating rule is stochastic. They inherit the computational power of CA and are used as models in a wide range of applications (see, for instance, the contributions in [32]). From a theoretic perspective, the main challenges concern the non-ergodicity of these dynamics for an infinite collection of interacting cells. Ergodicity means the non-dependence of the long-time behavior on the initial probability distribution and the convergence in law towards a unique stationary probability distribution (see [34] for details and references). Non-ergodicity is related to *critical phenomena* and it is sometimes referred to as *dynamical phase transition*.

Strong relations exist between PCA and the general equilibrium statistical mechanics framework [16, 23, 36]. Important issues are related to the interplay between disordered global states and ordered phases (*emergence of organized global states, phase transition*) [28]. Although, PCA initial interest arose in the framework of Statistical Physics, in the recent literature many different applications of PCA have been proposed. In particular it is notable to remark that a natural context in which the PCA main ideas are of interest is that of evolutionary games [29–31].

PCA dynamics are naturally defined on an infinite lattice. Given a local stochastic updating rule, one has to face the usual problems about the connections between the PCA dynamics on a finite subpart of the lattice and the dynamics on the infinite lattice. In particular, it was stated in [17] for translation-invariant infinite volume PCA with *positive rates*¹, that the law of the trajectories, starting from any stationary translation-invariant distribution, is the Boltzmann–Gibbs distribution for some space-time associated potential. Thus phase transition for the space-time potential is intimately related to the PCA dynamical phase transition.

Moreover, see [14, Proposition 2.2], given a translation-invariant PCA dynamics, if there exists one translation-invariant stationary distribution which is a Gibbs measure with respect to some potential on the lattice, then all the associated translation-invariant stationary

¹A PCA is said to be with *positive rates* if the local updating rule is a distribution giving positive probability to any cell-state.

distributions are Gibbs with respect to the the same potential.

In this paper we shall consider a particular class of PCA, called *reversible* PCA, which are reversible with respect to a Gibbs-like measure defined via a translation invariant multi-body potential. In this framework we shall study the zero and low-temperature phase diagram of such an equilibrium statistical mechanics-like system, whose phases are related to the stationary measures of the original PCA.

We shall now first briefly recall formally the definitions of Cellular Automata and Probabilistic Cellular Automata and then describe the main results of the paper.

1.1. Cellular Automata

Cellular Automata are defined via a local deterministic evolution rule. Let $\Lambda \subset \mathbb{Z}^d$ be a finite cube with periodic boundary conditions.

Associate with each site $i \in \Lambda$ (also called *cell*) the state variable $\sigma_i \in \mathcal{S}_0$, where \mathcal{S}_0 is a finite single-site space and denote by $\Omega := \mathcal{S}_0^\Lambda$ the *state space*. Any $\sigma \in \Omega$ is called a *state* or *configuration* of the system.

In order to define the evolution rule we consider I , a subset of the torus Λ , and a function $f_I : \mathcal{S}_0^I \rightarrow \mathcal{S}_0$ depending on the state variables in I . We also introduce the shift Θ_i on the torus, for any $i \in \Lambda$, defined as the map $\Theta_i : \Omega \rightarrow \Omega$

$$(\Theta_i \sigma)_j = \sigma_{i+j}. \quad (1.1)$$

The configuration σ at site j shifted by i is equal to the configuration at site $i + j$. For example (see figure 1.1) set $j = 0$, then the value of the spin at the origin 0 will be mapped to site i . The *Cellular Automaton* on Ω with rule f_I is the sequence $\sigma(0), \sigma(1), \dots, \sigma(t)$, for t a positive integer, of states in Ω satisfying the following (deterministic) rule:

$$\sigma_i(t) = f_I(\Theta_i \sigma(t-1)) \quad (1.2)$$

for all $i \in \Lambda$ and $t \geq 1$.

Note the local and parallel character of the evolution: the value $\sigma_i(t+1)$, for all $i \in \Lambda$, of all the state variables at time $t+1$ depend on the value of the state variables at time t (parallel evolution) associated only with the sites in $i + I$ (locality).

1.2. Probabilistic Cellular Automata

The stochastic version of Cellular Automata is called *Probabilistic Cellular Automata* (PCA). We consider a probability distribution $f_\sigma : \mathcal{S}_0 \rightarrow [0, 1]$ depending on the state σ restricted to I ; we drop the dependence on I in the notation for future convenience. A Probabilistic Cellular Automata is the Markov chain $\sigma(0), \sigma(1), \dots, \sigma(t)$ on Ω with transition matrix

$$p(\sigma, \eta) = \prod_{i \in \Lambda} f_{\Theta_i \sigma}(\eta_i) \quad (1.3)$$

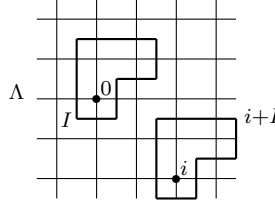


Figure 1.1: Schematic representation of the action of the shift Θ_i defined in (1.1).

for $\sigma, \eta \in \Omega$. We remark that f depends on $\Theta_i \sigma$ only via the neighborhood $i + I$. Note that, as in the deterministic case, the character of the evolution is local and parallel.

1.3. Description of the problem and results

Under suitable hypotheses on the probability distribution f_σ , for Λ finite, the Markov chain is irreducible and aperiodic, so that a unique stationary probability measure exists. On the other hand, irreducible and aperiodic PCA are in general not reversible. As already proven in [18, 21, 34] there exists a class of PCA which are reversible with respect to a Gibbs-like probability measure [14, Proposition 3.1] and, hence, they admit a sort of Hamiltonian. These models will be called *reversible PCA* (see [24, Section 3.5] for more details).

From the results in [14], see for instance Proposition 3.3 therein, it is possible to deduce that these Gibbs-like measures are either stationary or two-periodic for the PCA. Therefore it is quite natural to compare the behavior of these distributions to the one of the statistical mechanics counterpart.

Moreover, it is worth mentioning that also non-equilibrium properties of the PCA dynamics have been widely investigated. In [25], in the attractive reversible case and in absence of phase transition, the equivalence between an equilibrium weak-mixing condition and the convergence towards a unique equilibrium state with exponential speed was proven. In [1, 7–9, 27] the metastable behavior of a certain class of reversible PCA has been analyzed. In this framework the remarkable interest of a particular reversible PCA has been pointed out, called the cross PCA (see Section 3). It is a two-dimensional reversible PCA in which the updating rule of a cell depends on the status of the five cells forming a cross centered at the cell itself. In this model, the future state of the spin at a given cell depends also on the present value of such a spin. This effect will be called *self-interaction* and its weight in the updating rule will be called *self-interaction intensity*.

In [10] the analogies between the metastable behavior of the cross PCA and the Blume–Capel model [2, 3, 5] have been pointed out. Starting from [7], it has been heuristically argued that from a metastability perspective, the cross model behaves like the Blume–Capel one once the checkerboard configuration and the self-interaction intensity of the cross model

are identified with the empty configuration and the chemical potential of the Blume–Capel one [12].

In this paper we shall investigate this analogy further from an equilibrium point of view. We study the low-temperature² phase diagram of the Gibbs-like measure associated with the cross PCA which, as explained above, is strictly connected to the structure of the stationary states of the PCA. This is a very difficult task, since the microscopic interaction is described by a Hamiltonian in which coupling constants associated with all the multi-body potentials that can be constructed inside a five site cross are present. As a first step we shall discuss the zero-temperature phase diagram, namely, the structure of the ground states of the system, and we will show that the analogy with the Blume–Capel model is still strict. The second step will be the study of how the phase diagram changes when the temperature is fixed to a small positive value. In this case we will see that great differences, at least at the level of the Mean Field approximation, between the Blume–Capel and the cross PCA case will emerge.

One of the distinguishing features of the Blume–Capel model is the presence of a triple point in the zero-temperature phase diagram corresponding to zero chemical potential and magnetic field. In this point the three ground states (homogeneous plus, minus, and lacuna state) coexist (see, for instance, [33, Fig. 1]). It was proven in [4, 33] that this triple point moves toward the region with positive chemical potential when the temperature is positive and small. This is an entropy effect explained in [33].

In the present paper for the cross PCA model we prove a similar structure for the zero-temperature phase diagram: the triple point is at zero self-interaction intensity and magnetic field. At this point the four ground states (homogeneous plus, minus, even checkerboard, and odd checkerboard) coexist. Due to the presence of four coexisting ground states, an entropy argument similar to the one developed for the Blume–Capel model suggests that the position of the triple point is not affected by a small positive temperature [8, Section 2.4]. In this paper we approach the problem also from a Mean Field point of view and we obtain a result consistent with this conjecture.

The paper is organized as follows. In Section 2 we introduce the reversible Probabilistic Cellular Automata and discuss some general properties. In Section 3 we introduce the cross PCA and discuss its Hamiltonian. In particular we study its ground states and draw the zero temperature phase diagram. In Section 4.1 we study the phase diagram of the cross PCA in the framework of the Mean Field approximation. Finally, we summarize our conclusions in Section 5. The technical details of the painstaking computations we had to perform have

²Note that in the case of reversible PCA the use of the word temperature is misleading since the stationary measure is not precisely a Gibbs one. But, as it will be discussed in Section 2.1, a parameter playing a similar role can be introduced.

been relegated to the Appendix.

2. Reversible Probabilistic Cellular Automata

In this section we shall introduce reversible Probabilistic Cellular Automata and discuss some general results on their Hamiltonian.

2.1. Reversible Probabilistic Cellular Automata

A class of *reversible* PCA can be obtained by choosing $\Omega = \{-1, +1\}^\Lambda$, and

$$f_{\sigma;h}(s) = \frac{1}{2} \left\{ 1 + s \tanh \left[\beta \left(\sum_{j \in \Lambda} k(j) \sigma_j + h \right) \right] \right\} \quad (2.4)$$

for all $s \in \{-1, +1\}$ where $T \equiv 1/\beta > 0$ and $h \in \mathbb{R}$ are called *temperature* and *magnetic field*. $k : \mathbb{Z}^2 \rightarrow \mathbb{R}$ is such that its support is a subset of Λ and $k(j) = k(j')$ whenever $j, j' \in \Lambda$ are symmetric with respect to the origin. Recall that, by definition, the support of the function k is the subset of Λ where the function k is different from zero. With the notation introduced above, the set I is the support of the function k .

Recall that Λ is a finite torus, namely, periodic boundary conditions are considered throughout this paper. It is not difficult to prove [18, 21] that the above specified PCA dynamics is reversible with respect to the finite-volume Gibbs-like measure³

$$\mu_{\beta,h}(\sigma) = \frac{1}{Z_\beta} e^{-\beta G_{\beta,h}(\sigma)} \quad (2.5)$$

with *Hamiltonian*

$$G_{\beta,h}(\sigma) = -h \sum_{i \in \Lambda} \sigma_i - \frac{1}{\beta} \sum_{i \in \Lambda} \log \cosh \left[\beta \left(\sum_{j \in \Lambda} k(j-i) \sigma_j + h \right) \right] \quad (2.6)$$

and *partition function*

$$Z_{\beta,h} = \sum_{\eta \in \Omega} e^{-\beta G_{\beta,h}(\eta)} \quad (2.7)$$

In other words, in this case the detailed balance equation

$$p(\sigma, \eta) e^{-\beta G_{\beta,h}(\sigma)} = e^{-\beta G_{\beta,h}(\eta)} p(\eta, \sigma)$$

³This statement, with some care, can be extended to non-periodic boundaries [14]. For finite lattice and periodic boundary conditions the finite-volume Gibbs distribution is the unique reversible one (our framework). For finite lattice and fixed deterministic non-periodic boundary conditions, the finite-volume Gibbs distribution differs from the unique reversible one; differences are somehow localized close to the boundary .

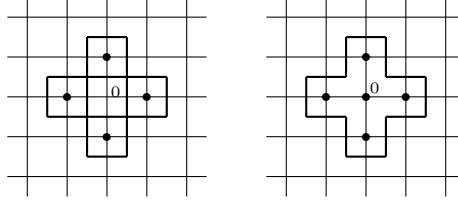


Figure 2.2: Schematic representation of the nearest neighbor (left) and cross (right) models.

is satisfied thus the probability measure $\mu_{\beta,h}$ is stationary for the PCA.

Note that different reversible PCA models can be specified by choosing different functions k . In particular the support I of such a function can be varied. The generality of this PCA family among the reversible one was remarked in Section 4.1.1 in [24]. Common choices are the *nearest neighbor PCA* [8] obtained by choosing the support of k as the set of the four sites neighboring the origin and the *cross PCA* [9] obtained by choosing the support of k as the set made of the origin and its four neighboring sites (see figure 2.2).

2.2. Connection with statistical mechanics stochastic systems

The interest of reversible PCA has already been discussed above. In this section we recall an interesting connection between reversible PCA and statistical mechanics lattice models [15] and [26, Section 2.4.2].

Consider a statistical mechanics model on the torus Λ (periodic boundary conditions) with configuration space $\Omega = \{-1, +1\}^\Lambda$ and Hamiltonian

$$F(\sigma) = -\frac{1}{2} \sum_{i,j \in \Lambda} J_{ij} \sigma_i \sigma_j - h \sum_{i \in \Lambda} \sigma_i$$

with $h \in \mathbb{R}$ and J_{ij} symmetrical and translationally invariant, that is $J_{ij} = J_{ji}$ and $J_{ij} = J_{i+s,j+s}$ for all $s \in \mathbb{Z}^2$. The equilibrium properties of the model at inverse temperature β are described by the finite-volume Gibbs measure $\nu_\beta(\sigma) = \exp\{-\beta F(\sigma)\} / \sum_{\eta \in \mathcal{S}} \exp\{-\beta F(\eta)\}$.

The stochastic version of the model is a discrete time Markov chain $\sigma(0), \sigma(1), \dots, \sigma(t)$ such that its stationary measure is equal to the equilibrium Gibbs measure ν_β . This can be achieved by choosing different transition matrices in the definition of the Markov chain. A very celebrated choice is the so-called *heat-bath (Glauber)* dynamics: at each time $t \in \mathbb{N}$ choose uniformly at random (with probability $1/|\Lambda|$) a site $i \in \Lambda$ and let $\sigma_i(t) = s$ with probability $f_{\Theta_i \sigma(t-1)}^{\text{HB}}(s)$ where

$$f_\sigma^{\text{HB}}(s) = \frac{\exp\{-\beta H(s\sigma_{\Lambda \setminus \{0\}})\}}{\exp\{-\beta H(s\sigma_{\Lambda \setminus \{0\}})\} + \exp\{-\beta H(-s\sigma_{\Lambda \setminus \{0\}})\}}$$

for any $\sigma \in \Omega$, where $\sigma_{\Lambda \setminus \{0\}}$ denotes the restriction of the configuration σ on $\Lambda \setminus \{0\}$. We have that

$$\begin{aligned} f_{\sigma}^{\text{HB}}(s) &= \frac{1}{1 + \exp\{\beta[H(s\sigma_{\Lambda \setminus \{0\}}) - H(-s\sigma_{\Lambda \setminus \{0\}})]\}} = \frac{1}{1 + \exp\{\beta[-2s(\sum_{j \in \Lambda} J_{0j}\sigma_j + h)]\}} \\ &= \frac{1}{2} \left\{ 1 + s \tanh \left[\beta \left(\sum_{j \in \Lambda} J_{0j}\sigma_j + h \right) \right] \right\} \end{aligned}$$

which is in the form (2.4).

Summing up, by implementing in a parallel fashion the heat-bath rates of a statistical mechanics lattice model, a reversible PCA is obtained. Notice that the stationary measure of the reversible PCA obtained is different from that of the starting statistical mechanics model. Then, an interesting question arises immediately: are there connections between the phase diagram of the starting statistical mechanics model and that of the resulting reversible PCA? This question is one of the problems which is addressed in this paper. We recall that a similar question has been posed in [8] in connection with metastability phenomena.

2.3. Low temperature behavior of the reversible PCA Hamiltonian

The stationary measure $\mu_{\beta,h}$ introduced above looks like a finite-volume Gibbs measure with Hamiltonian $G_{\beta,h}(\sigma)$ (see (2.6)). It is worth noting that $G_{\beta,h}$ cannot be thought as a proper statistical mechanics Hamiltonian since it depends on the temperature $1/\beta$. On the other hand the low-temperature behavior of the stationary measure of the PCA can be guessed by looking at the function

$$H_h(\sigma) = \lim_{\beta \rightarrow \infty} G_{\beta,h}(\sigma) = -h \sum_{i \in \Lambda} \sigma_i - \sum_{i \in \Lambda} \left| \sum_{j \in \Lambda} k(j-i)\sigma_j + h \right| \quad (2.8)$$

The absolute minima of the function H_h are called *ground states* of the stationary measure for the reversible PCA.

Following [7], the difference between the Hamiltonian $G_{\beta,h}$ and its zero temperature limit H_h can be computed. We have that

$$G_{\beta,h}(\sigma) - H_h(\sigma) = -\frac{1}{\beta} \sum_{i \in \Lambda} \log \left(1 + \exp \left\{ -2\beta \left| \sum_{j \in \Lambda} k(j-i)\sigma_j + h \right| \right\} \right) + \frac{1}{\beta} |\Lambda| \log(2) \quad (2.9)$$

for each $\beta > 0$ and $\sigma \in \Omega$. Indeed,

$$\begin{aligned} G_{\beta,h}(\sigma) - H_h(\sigma) &= -\frac{1}{\beta} \sum_{i \in \Lambda} \log \cosh \left[\beta \left(\sum_{j \in \Lambda} k(j-i) \sigma_j + h \right) \right] + \sum_{i \in \Lambda} \left| \sum_{j \in \Lambda} k(j-i) \sigma_j + h \right| \\ &= -\frac{1}{\beta} \sum_{i \in \Lambda} \left\{ \log \cosh \left[\beta \left(\sum_{j \in \Lambda} k(j-i) \sigma_j + h \right) \right] \right. \\ &\quad \left. - \log \exp \left[\beta \left| \sum_{j \in \Lambda} k(j-i) \sigma_j + h \right| \right] \right\} \end{aligned}$$

Hence

$$G_{\beta,h}(\sigma) - H_h(\sigma) = -\frac{1}{\beta} \sum_{i \in \Lambda} \log \frac{\exp \left[\beta \left| \sum_{j \in \Lambda} k(j-i) \sigma_j + h \right| \right] + \exp \left[-\beta \left| \sum_{j \in \Lambda} k(j-i) \sigma_j + h \right| \right]}{2 \exp \left[\beta \left| \sum_{j \in \Lambda} k(j-i) \sigma_j + h \right| \right]}$$

which yields (2.9).

3. The cross PCA

In this paper we shall study the phase diagram of the Gibbs-like measure associated to the *cross PCA*. More precisely, we shall that $k(j) = 0$ if j is neither the origin nor one of its nearest neighbors, i.e. in the cross I . In this case, since k has to be symmetric with respect to the origin, the probability measure $f_{\sigma,h}$ has to be

$$f_{\sigma,h}(s) = \frac{1}{2} \left\{ 1 + s \tanh \left[\beta \left(k_0 \sigma_0 + k_1 [\sigma_{e_1} + \sigma_{-e_1}] + k_2 [\sigma_{e_2} + \sigma_{-e_2}] + h \right) \right] \right\}$$

where e_1 and e_2 are unit vectors parallel to the coordinate axes of the lattice and $k_0, k_1, k_2 \in \mathbb{R}$. The constant k_0 is the *self-interaction intensity*. To sum up, the *cross PCA* is a family of PCA dynamics parameterized by k_0, k_1, k_2, β, h .

Note that for the cross model the Hamiltonian $G_{\beta,h}$ defining the stationary Gibbs-like measure is given by

$$\begin{aligned} G_{\beta,h}(\sigma) &= -h \sum_{i \in \Lambda} \sigma_i - \frac{1}{\beta} \sum_{i \in \Lambda} \log \cosh \left[\beta \left(k_0 \sigma_i + k_1 [\sigma_{i+e_1} + \sigma_{i-e_1}] \right. \right. \\ &\quad \left. \left. + k_2 [\sigma_{i+e_2} + \sigma_{i-e_2}] + h \right) \right] \end{aligned} \quad (3.10)$$

The Hamiltonian can be rewritten as

$$G_{\beta,h}(\sigma) = \sum_{i \in \Lambda} G_{\beta,h,i}(\sigma) \quad (3.11)$$

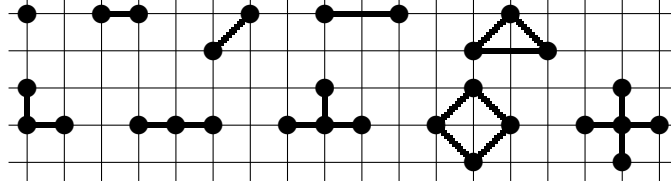


Figure 3.3: Schematic representation of the coupling constants: from the left to the right and from the top to the bottom the couplings J , $J_{\langle 1 \rangle}$, $J_{\langle \rangle}$, $J_{\langle \langle \rangle \rangle_1}$, J_{Δ_1} , J_{\perp} , J_{\sim_1} , J_{\perp_1} , J_{\diamond} , and J_{+} are depicted.

where

$$G_{\beta,h,i}(\sigma) = G_{\beta,h}^0(\Theta_i \sigma) \quad (3.12)$$

and

$$\begin{aligned} G_{\beta,h}^0(\sigma) = & -\frac{1}{5}h[\sigma_0 + \sigma_{e_1} + \sigma_{-e_1} + \sigma_{e_2} + \sigma_{-e_2}] \\ & -\frac{1}{\beta} \log \cosh\{\beta(k_0\sigma_0 + k_1[\sigma_{e_1} + \sigma_{-e_1}] + k_2[\sigma_{e_2} + \sigma_{-e_2}] + h)\} \end{aligned} \quad (3.13)$$

Note that, for any $i \in \Lambda$, $G_{\beta,h,i}$ is the contribution of the cross centered at the site i of the torus Λ to the Hamiltonian of the system.

3.1. Coupling constants for the Hamiltonian of the cross PCA

In statistical mechanics systems the Hamiltonian is usually written as a sum of potentials each of them being the product of the spin variables over some subset of the lattice multiplied by a constant called *coupling constant*. For any $\sigma \in \Omega$ and any $I \subset \Lambda$ we set

$$\sigma_I = \prod_{i \in I} \sigma_i \quad (3.14)$$

In this section we prove that the Hamiltonian (3.10) for the cross PCA can be written in the form

$$\begin{aligned} G_{\beta,h}(\sigma) = & -J \sum_{i \in \Lambda} \sigma_i - J_{\langle 1 \rangle} \sum_{\langle 1 \rangle} \sigma_{\langle 1 \rangle} - J_{\langle 2 \rangle} \sum_{\langle 2 \rangle} \sigma_{\langle 2 \rangle} - J_{\langle \rangle} \sum_{\langle \rangle} \sigma_{\langle \rangle} - J_{\langle \langle \rangle \rangle_1} \sum_{\langle \langle \rangle \rangle_1} \sigma_{\langle \langle \rangle \rangle_1} \\ & - J_{\langle \langle \rangle \rangle_2} \sum_{\langle \langle \rangle \rangle_2} \sigma_{\langle \langle \rangle \rangle_2} - J_{\Delta_1} \sum_{\Delta_1} \sigma_{\Delta_1} - J_{\Delta_2} \sum_{\Delta_2} \sigma_{\Delta_2} - J_{\perp} \sum_{\perp} \sigma_{\perp} - J_{\sim_1} \sum_{\sim_1} \sigma_{\sim_1} \\ & - J_{\sim_2} \sum_{\sim_2} \sigma_{\sim_2} - J_{\perp_1} \sum_{\perp_1} \sigma_{\perp_1} - J_{\perp_2} \sum_{\perp_2} \sigma_{\perp_2} - J_{\diamond} \sum_{\diamond} \sigma_{\diamond} - J_{+} \sum_{+} \sigma_{+} \end{aligned} \quad (3.15)$$

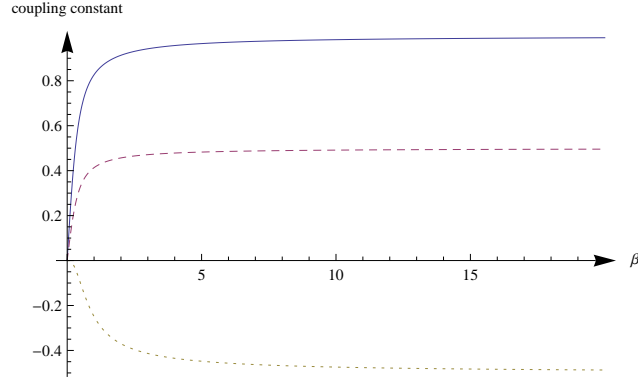


Figure 3.4: The coupling constants $J_{\langle \rangle}$ (solid), $J_{\langle \rangle \rangle \rangle \rangle_1} = J_{\langle \rangle \rangle \rangle \rangle_2}$ (dashed), and J_{\diamond} (dotted). are plotted at $h = 0$, $k_0 = 0$, and $k_1 = k_2 = 1$ as a function of β .

where the meaning of each term is illustrated in figure 3.3 and its expression as function of h , β , k_0 , k_1 , and k_2 is given in the Appendix A. Note that 1 and 2 mean, respectively, oriented along the 1 and the 2 coordinate direction (namely, horizontal and vertical).

We calculate the coefficients J 's by using [13, equations (6) and (7)] (see also [19, equations (3.1) and (3.2)] and [11]). More precisely, given $f : \{-1, +1\}^V \rightarrow \mathbb{R}$, with $V \subset \mathbb{Z}^2$ finite, we have that for any $\sigma \in \{-1, +1\}^V$

$$f(\sigma) = \sum_{I \subset V} C_I \prod_{i \in I} \sigma_i \quad (3.16)$$

with the coefficients C_I 's given by

$$C_I = \frac{1}{2^{|V|}} \sum_{\sigma \in \{-1, +1\}^V} f(\sigma) \prod_{i \in I} \sigma_i \quad (3.17)$$

By expanding the function $-G_{\beta, h}^0$ defined in the cross centered at the origin we obtain, by exploiting the symmetry of the cross, the seventeen different coefficients J_{\bullet}^0 , $J_{\circ_1}^0$, $J_{\circ_2}^0$, $J_{\langle \rangle_1}^0$, $J_{\langle \rangle_2}^0$, $J_{\langle \rangle \rangle \rangle \rangle_1}^0$, $J_{\langle \rangle \rangle \rangle \rangle_2}^0$, $J_{\Delta_1}^0$, $J_{\Delta_2}^0$, J_{\perp}^0 , $J_{\sim_1}^0$, $J_{\sim_2}^0$, $J_{\perp_1}^0$, $J_{\perp_2}^0$, J_{\diamond}^0 , and J_{+}^0 whose meaning is the same as for the J 's introduced above (see also figure 3.3) but for the single site coefficients J_{\bullet}^0 , $J_{\circ_1}^0$, and $J_{\circ_2}^0$ which refer, respectively, to the center and to the peripheral sites of the cross on the 1 and on the 2 direction. The coefficients we get are listed in the Appendix A.

By exploiting, now, the translational invariance of the cross PCA Hamiltonian $G_{\beta, h}$ we have that

$$\begin{aligned} J_{\bullet} &= J_{\bullet}^0 + 2J_{\circ_1}^0 + 2J_{\circ_2}^0, & J_{\langle \rangle_1} &= 2J_{\langle \rangle_1}^0, & J_{\langle \rangle_2} &= 2J_{\langle \rangle_2}^0, & J_{\langle \rangle} &= 2J_{\langle \rangle}^0, & J_{\langle \rangle \rangle \rangle \rangle_1} &= J_{\langle \rangle \rangle \rangle \rangle_1}^0, \\ J_{\langle \rangle \rangle \rangle \rangle_2} &= J_{\langle \rangle \rangle \rangle \rangle_2}^0, & J_{\Delta_1} &= J_{\Delta_1}^0, & J_{\Delta_2} &= J_{\Delta_2}^0, & J_{\perp} &= J_{\perp}^0, & J_{\sim_1} &= J_{\sim_1}^0, \\ J_{\sim_2} &= J_{\sim_2}^0, & J_{\perp_1} &= J_{\perp_1}^0, & J_{\perp_2} &= J_{\perp_2}^0, & J_{\diamond} &= J_{\diamond}^0, & J_{+} &= J_{+}^0 \end{aligned} \quad (3.18)$$

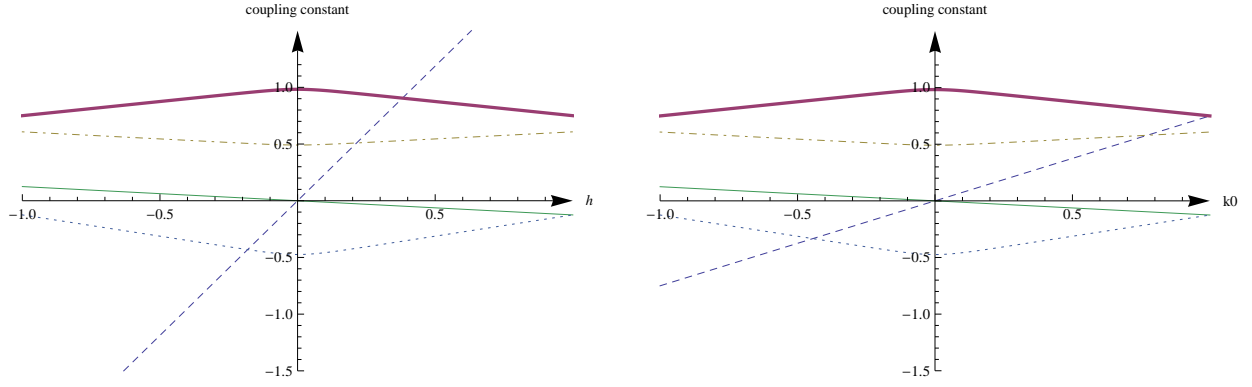


Figure 3.5: Left: the coupling constants J (dashed), $J_{\langle\langle\rangle\rangle}$ (solid thick), $J_{\langle\langle\rangle\rangle\langle\langle\rangle\rangle_1} = J_{\langle\langle\rangle\rangle\langle\langle\rangle\rangle_2}$ (dot-dashed), $J_{\Delta_1} = J_{\Delta_2}$ (solid thin), and J_{\diamond} (dotted) are plotted at $\beta = 10$, $k_0 = 0$, and $k_1 = k_2 = 1$ as a function of h . Right: the coupling constants $J_{\langle\rangle_1} = J_{\langle\rangle_2}$ (dashed), $J_{\langle\langle\rangle\rangle}$ (solid thick), $J_{\langle\langle\rangle\rangle\langle\langle\rangle\rangle_1} = J_{\langle\langle\rangle\rangle\langle\langle\rangle\rangle_2}$ (dot-dashed), $J_{\perp_1} = J_{\perp_2}$ (solid thin), and J_{\diamond} (dotted) are plotted at $\beta = 10$, $h = 0$, and $k_1 = k_2 = 1$ as a function of k_0 .

The coupling constants J 's depend on the parameters of the model, namely, β , h , k_0 , k_1 , and k_2 , see also the explicit expressions given in Appendix A. To give an idea of their typical values we plot some of them in the figures 3.4 and 3.5.

In figure 3.4 we plot the coupling constants at $h = 0$, $k_0 = 0$, and $k_1 = k_2 = 1$ as a function of β . Note that with such a choice of the parameters the sole non zero couplings are $J_{\langle\langle\rangle\rangle}$, $J_{\langle\langle\rangle\rangle\langle\langle\rangle\rangle_1}$, $J_{\langle\langle\rangle\rangle\langle\langle\rangle\rangle_2}$, and J_{\diamond} . Moreover, since $k_1 = k_2$, it turns out that $J_{\langle\langle\rangle\rangle\langle\langle\rangle\rangle_1} = J_{\langle\langle\rangle\rangle\langle\langle\rangle\rangle_2}$.

In figure 3.5 on the left we plot the coupling constants at $\beta = 10$, $k_0 = 0$, and $k_1 = k_2 = 1$ as a function of h . Note that, from the graphs in figure 3.4, it results that the coupling constants are approximatively constant for $\beta \geq 5$. Note that with such a choice of the parameters the sole non zero couplings are J , $J_{\langle\langle\rangle\rangle}$, $J_{\langle\langle\rangle\rangle\langle\langle\rangle\rangle_1}$, $J_{\langle\langle\rangle\rangle\langle\langle\rangle\rangle_2}$, J_{Δ_1} , J_{Δ_2} , and J_{\diamond} . Moreover, since $k_1 = k_2$, it turns out that $J_{\langle\langle\rangle\rangle\langle\langle\rangle\rangle_1} = J_{\langle\langle\rangle\rangle\langle\langle\rangle\rangle_2}$ and $J_{\Delta_1} = J_{\Delta_2}$.

In figure 3.5 on the right we plot the coupling constants at $\beta = 10$, $h = 0$, and $k_1 = k_2 = 1$ as a function of k_0 . Note that with such a choice of the parameters the sole non zero couplings are $J_{\langle\rangle_1}$, $J_{\langle\rangle_2}$, $J_{\langle\langle\rangle\rangle}$, $J_{\langle\langle\rangle\rangle\langle\langle\rangle\rangle_1}$, $J_{\langle\langle\rangle\rangle\langle\langle\rangle\rangle_2}$, J_{\perp_1} , J_{\perp_2} , and J_{\diamond} . Moreover, since $k_1 = k_2$, it turns out that $J_{\langle\rangle_1} = J_{\langle\rangle_2}$, $J_{\langle\langle\rangle\rangle\langle\langle\rangle\rangle_1} = J_{\langle\langle\rangle\rangle\langle\langle\rangle\rangle_2}$ and $J_{\perp_1} = J_{\perp_2}$.

3.2. Ground states of the cross PCA

Assume that the side length of the torus Λ is an even number. Furthermore, we assume that $|k_0| < 2(k_1 + k_2)$ in order for the self-interaction not to be able to change the majority of the cross configuration. Recalling the definition of ground states given in Section 2.3, we have

that the ground states of the cross PCA are the absolute minima of the function

$$H_h(\sigma) = -h \sum_{i \in \Lambda} \sigma_i - \sum_{i \in \Lambda} \left| k_0 \sigma_i + k_1 [\sigma_{i+e_1} + \sigma_{i-e_1}] + k_2 [\sigma_{i+e_2} + \sigma_{i-e_2}] + h \right| \quad (3.19)$$

which can be rewritten as

$$H_h(\sigma) = \sum_{i \in \Lambda} H_{h,i}(\sigma) \quad (3.20)$$

where

$$H_{h,i}(\sigma) = - \left[\frac{1}{5} h [\sigma_i + \sigma_{i+e_1} + \sigma_{i-e_1} + \sigma_{i+e_2} + \sigma_{i-e_2}] + |k_0 \sigma_i + k_1 [\sigma_{i+e_1} + \sigma_{i-e_1}] + k_2 [\sigma_{i+e_2} + \sigma_{i-e_2}] + h| \right] \quad (3.21)$$

Remark that

$$\lim_{\beta \rightarrow \infty} G_{\beta,h,i}(\sigma) = H_{h,i}(\sigma)$$

for each $h \in \mathbb{R}$, $i \in \Lambda$, and $\sigma \in \Omega$. We also note that

$$H_h(\sigma) = H_{-h}(-\sigma) \quad (3.22)$$

for any $h \in \mathbb{R}$ and $\sigma \in \Omega$, where $-\sigma$ denotes the configuration obtained by flipping the sign of all the spins of σ . By (3.22) we can bound our discussion to the case $h \geq 0$ and deduce a posteriori the structure of the ground states for $h < 0$.

Moreover, we notice that, since H_h is in the form (3.20), a global minimum of H_h is realized by minimizing each $H_{h,i}(\sigma)$ for any $i \in \Lambda$.

We discuss the structure of the ground states of the cross PCA under the assumption $k_1, k_2 > 0$ and consider the following cases (see figure 3.6).

Case $h > 0$ and $k_0 \geq 0$. The minimum of $H_{h,i}$ is attained at the cross configuration having all the spins equal to plus one. Hence the unique absolute minimum of H_h is the configuration \mathbf{u} such that $\mathbf{u}(i) = +1$ for all $i \in \Lambda$.

Case $h > -k_0$ and $k_0 < 0$. If the spin at i is plus, since $h + k_0 > 0$, $H_{h,i}$ is then minimal provided all the other spins in the cross are equal to $+1$ and it is equal to $-h - |k_0 + 2(k_1 + k_2) + h|$. If the spin at i is minus, since $h - k_0 > 0$, $H_{h,i}$ is then minimal provided all the other spins in the cross are equal to $+1$ and it is equal to $-3h/5 - |-k_0 + 2(k_1 + k_2) + h|$. Is not difficult to prove that

$$-h - |k_0 + 2(k_1 + k_2) + h| \leq -3h/5 - |-k_0 + 2(k_1 + k_2) + h| \text{ if and only if } h \geq -5k_0$$

We can then conclude that in the region $k_0 < 0$ and $h > -5k_0$ the ground state of the cross PCA is the configuration \mathbf{u} .

In the region $k_0 < 0$ and $0 < h < -5k_0$ the situation is more complicated and we expect that the line $h = -k_0$ is the boundary between the regions where the ground states are respectively \mathbf{u} and the pair \mathbf{c}_e and \mathbf{c}_o with \mathbf{c}_e the checkerboard configuration with pluses on the even sub-lattice of Λ and minuses on its complement, while \mathbf{c}_o is the corresponding spin-flipped configuration. Indeed, we can write $H_h(\mathbf{u}) = -|\Lambda|[h + |k_0 + 2k_1 + 2k_2 + h|]$ and, hence,

$$H_h(\mathbf{u}) = \begin{cases} -|\Lambda|[k_0 + 2(k_1 + k_2) + 2h] & \text{if } k_0 + 2k_1 + 2k_2 + h > 0 \\ -|\Lambda|[-k_0 - 2(k_1 + k_2)] & \text{if } k_0 + 2k_1 + 2k_2 + h < 0 \end{cases}$$

Moreover, recalling $k_0 < 0$, $H_h(\mathbf{c}_e) = H_h(\mathbf{c}_o) = -(|\Lambda|/2)[|k_0 - 2k_1 - 2k_2 + h| + |-k_0 + 2k_1 + 2k_2 + h|] = -(|\Lambda|/2)[|k_0 - 2k_1 - 2k_2 + h| + (-k_0 + 2k_1 + 2k_2 + h)]$. Hence,

$$H_h(\mathbf{c}_e) = H_h(\mathbf{c}_o) = \begin{cases} -|\Lambda|h & \text{if } k_0 - 2k_1 - 2k_2 + h > 0 \\ -|\Lambda|[-k_0 + 2k_1 + 2k_2] & \text{if } k_0 - 2k_1 - 2k_2 + h < 0 \end{cases}$$

From these explicit expressions, by discussing separately the three cases $h > -k_0 + 2(k_1 + k_2)$, $-k_0 + 2(k_1 + k_2) > h > -k_0 - 2(k_1 + k_2)$, and $-k_0 - 2(k_1 + k_2) > h$, it follows that $H_h(\mathbf{c}_e) = H_h(\mathbf{c}_o) < H_h(\mathbf{u})$ if and only if $h + k_0 < 0$.

We now discuss those cases in which the external field h is equal to zero. We first note that in this case the term $H_{h,i}$ reduces to

$$H_{0,i}(\sigma) = -|k_0\sigma_i + k_1[\sigma_{i+e_1} + \sigma_{i-e_1}] + k_2[\sigma_{i+e_2} + \sigma_{i-e_2}]| \quad (3.23)$$

Case $h = 0$ and $k_0 > 0$. The minimum of $H_{0,i}$ is attained at the cross configuration having all the spins equal to plus one or all equal to minus one. Hence the set of ground states is made of the two configurations \mathbf{u} and \mathbf{d} with this last one such that $\mathbf{d}(i) = -1$ for all $i \in \Lambda$.

Case $h = 0$ and $k_0 = 0$. The minimum of $H_{0,i}$ is attained at the cross configuration having all the spins equal to plus one or all equal to minus one on the neighbors of the center and with the spin at the center which can be, in any case, either plus or minus. Hence the set of ground states is made of the four configurations \mathbf{u} , \mathbf{d} , \mathbf{c}_e , and \mathbf{c}_o .

Case $h = 0$ and $k_0 < 0$. The minimum of $H_{0,i}$ is attained at the cross configuration having the spin at the center equal to plus one and the others equal to minus one and at the spin-flipped cross configuration. Hence the set of ground states is made of the two configurations \mathbf{c}_e and \mathbf{c}_o .

Case $h < 0$. The set of ground states can be easily discussed as for $h > 0$ by using the property (3.22).

3.3. Phase diagram

The goal of this paper is the study of the effect of the self-interaction parameter k_0 on the phase diagram of the Gibbs-like measure (2.5) with Hamiltonian (3.10) associated with the

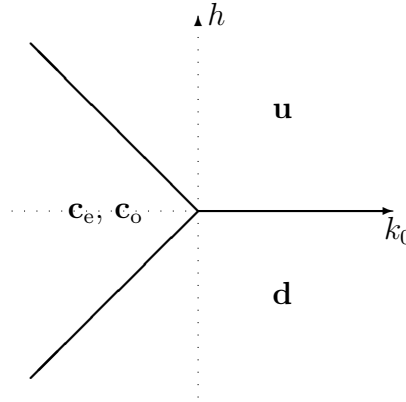


Figure 3.6: Expected zero temperature phase diagram of the stationary measure of the cross PCA. On the thick lines the ground states of the adjacent regions coexist. At the origin the four ground states coexist.

cross PCA. In other words we want to study how the ground states structure depicted in figure 3.6 is deformed when a small non-zero temperature is considered. One interesting feature is the connection with the well know Blume–Capel model which has been widely discussed in the introduction, see Section 1.3.

As recalled in Section 1.3 such a phase diagram is strictly connected with the structure of the stationary states of the PCA. On this subject very few rigorous results have been established:

- it has been remarked in [21] and in [14, Remark 4.1] and proven more accurately [24, Th. 4.2.5 Section 4.2.2, Proposition 4.3.4 Section 4.3.3] that at $h = k_0 = 0$ the model can be decoupled into two independent systems defined on the even and on the odd part of the lattice and that the phase diagram is the same as that of two independent nearest-neighbor Ising models. The set of Gibbs distributions consists in the convex hull generated by the four Gibbs distributions respectively close to **u**, **d**, **c_e**, and **c_o** and obtained by taking those as boundary conditions and considering the thermodynamic limit.
- For $h = 0$, $k_1 \neq 0$, $k_2 \neq 0$ and for any k_0 , it has been proven in [14, Proposition 4.1] that for T smaller than a critical value, a phase transition for the Gibbs-like measure associated with the PCA occurs.

Consider, now, the three-dimensional space k_0 – h – T , where we recall $T = 1/\beta$ is the temperature. The rigorous results quoted above are related to some subparts of such a

space. What we want to do is to study the phase diagram in the whole space and precise which phases are at play. Obtaining rigorous results of this kind is an absolutely difficult task. In this paper we shall give an idea of the phase diagram in this space via Mean Field computations, see Section 4.1.

4. Mean Field phase diagram

In this section we shall study the phase diagram of the Gibbs-like measure associated with the cross PCA via a suitable Mean Field approximation.

4.1. The Mean Field free energy

The Mean Field approximation relies on considering non-correlated degrees of freedom. In other words the equilibrium density matrix ϱ_Λ is supposed to be factorized as the product of one-site transition matrices ϱ_x for each $x \in \Lambda$. Moreover, inspired by the structure of the ground states discussed above, we partition the squared torus Λ in its even and odd components Λ_e and Λ_o , respectively, and assume that with each site of the even component is associated the single site matrix ϱ_e and with each site of the odd component is associated the single site matrix ϱ_o . In other words we assume $\varrho_x = \varrho_e$ for $x \in \Lambda_e$ and $\varrho_x = \varrho_o$ for $x \in \Lambda_o$, that is to say we assume the density matrix to be in the form

$$\varrho_\Lambda(\sigma) = \prod_{x \in \Lambda_e} \varrho_e(\sigma_x) \prod_{y \in \Lambda_o} \varrho_o(\sigma_y) \quad (4.24)$$

for any configuration $\sigma \in \Omega$. The next step is that of computing, under such assumption, the free energy [6]

$$f = \frac{1}{|\Lambda|} \left(U - \frac{1}{\beta} S \right) \quad (4.25)$$

where

$$U := \sum_{\sigma \in \Omega} \varrho_\Lambda(\sigma) G_{\beta, h}(\sigma) \quad \text{and} \quad S := - \sum_{\sigma \in \Omega} \varrho_\Lambda(\sigma) \log \varrho_\Lambda(\sigma) \quad (4.26)$$

are, respectively, the *internal energy* and the *entropy*.

We now compute the entropy under the Mean Field hypothesis. First of all we note that

$$-S = \sum_{\sigma \in \Omega} \prod_{x \in \Lambda_e} \varrho_e(\sigma_x) \prod_{y \in \Lambda_o} \varrho_o(\sigma_y) \log \left(\prod_{w \in \Lambda_e} \varrho_e(\sigma_w) \prod_{z \in \Lambda_o} \varrho_o(\sigma_z) \right)$$

and, hence,

$$-S = \sum_{w \in \Lambda_e} \sum_{\sigma \in \Omega} \prod_{x \in \Lambda_e} \varrho_e(\sigma_x) \prod_{y \in \Lambda_o} \varrho_o(\sigma_y) \log \varrho_e(\sigma_w) + \sum_{z \in \Lambda_o} \sum_{\sigma \in \Omega} \prod_{x \in \Lambda_e} \varrho_e(\sigma_x) \prod_{y \in \Lambda_o} \varrho_o(\sigma_y) \log \varrho_o(\sigma_z)$$

Finally, we get

$$-S = \frac{|\Lambda|}{2} \left(\sum_{s=\pm 1} \varrho_e(s) \log \varrho_e(s) + \sum_{s=\pm 1} \varrho_o(s) \log \varrho_o(s) \right) \quad (4.27)$$

We define now the *even* and the *odd site* magnetizations

$$m_e = \sum_{s=\pm 1} s \varrho_e(s) \quad \text{and} \quad m_o = \sum_{s=\pm 1} s \varrho_o(s) \quad (4.28)$$

Note that, recalling $\varrho_r(+1) + \varrho_r(-1) = 1$ for $r = e, o$, we have that

$$\varrho_r(+1) = \frac{1 + m_r}{2} \quad \text{and} \quad \varrho_r(-1) = \frac{1 - m_r}{2} \quad (4.29)$$

with $r = e, o$. By (4.27) and (4.29) we get, for the Mean Field entropy, the expression

$$\begin{aligned} -S = \frac{|\Lambda|}{2} \left\{ \frac{1 + m_e}{2} \log \frac{1 + m_e}{2} + \frac{1 - m_e}{2} \log \frac{1 - m_e}{2} \right. \\ \left. + \frac{1 + m_o}{2} \log \frac{1 + m_o}{2} + \frac{1 - m_o}{2} \log \frac{1 - m_o}{2} \right\} \end{aligned} \quad (4.30)$$

The computation of the internal energy in the Mean Field approximation is more delicate and the expansion for the Hamiltonian discussed in Section 3.1 will be used. First of all recall (4.26) and note that

$$U = \sum_{x \in \Lambda} \sum_{\sigma \in \Omega} \varrho_\Lambda(\sigma) G_{\beta, h, x}(\sigma) = \sum_{x \in \Lambda} \sum_{\substack{\sigma_y = \pm 1: \\ y \in C(x)}} \left(\prod_{y \in C(x)} \varrho_y(\sigma_y) \right) G_{\beta, h, x}(\sigma)$$

where we have used (3.11), set $C(x) := \{x, x + e_1, x - e_1, x + e_2, x - e_2\}$ for each $x \in \Lambda$, and recalled that $G_{\beta, h, x}(\sigma)$ depends only on the spins σ_y with $y \in C(x)$.

Now, since $0 = (0, 0) \in \Lambda_e$ and $(1, 0) \in \Lambda_o$, by exploiting the translation invariance of the Hamiltonian and the structure of the Mean Field transition matrices, we have that

$$U = \frac{|\Lambda|}{2} \left[\sum_{\substack{\sigma_y = \pm 1: \\ y \in C(0)}} \left(\prod_{y \in C(0)} \varrho_y(\sigma_y) \right) G_{\beta, h, 0}(\sigma) + \sum_{\substack{\sigma_y = \pm 1: \\ y \in C((1, 0))}} \left(\prod_{y \in C((1, 0))} \varrho_y(\sigma_y) \right) G_{\beta, h, (1, 0)}(\sigma) \right]$$

We finally get

$$U = \frac{|\Lambda|}{2} (u_e + u_o) \quad (4.31)$$

with

$$u_e = \sum_{\substack{\sigma_y = \pm 1: \\ y \in C(0)}} \left(\prod_{y \in C(0)} \varrho_y(\sigma_y) \right) G_{\beta, h, 0}(\sigma) \quad \text{and} \quad u_o = \sum_{\substack{\sigma_y = \pm 1: \\ y \in C((1, 0))}} \left(\prod_{y \in C((1, 0))} \varrho_y(\sigma_y) \right) G_{\beta, h, (1, 0)}(\sigma)$$

The coefficients J^0 's introduced below (3.17) and listed in the Appendix A, have been obtained by expanding the function $G_{\beta,h}^0$. This remark and a straightforward computation yield to the equation

$$\begin{aligned} -u_e = & J_{\bullet}^0 m_e + 2(J_{o_1}^0 + J_{o_2}^0) m_o + 2(J_{\langle 1 \rangle}^0 + J_{\langle 2 \rangle}^0) m_e m_o + (4J_{\langle \rangle}^0 + J_{\langle \langle \rangle \rangle_1}^0 + J_{\langle \langle \rangle \rangle_2}^0) m_o^2 \\ & + 2(J_{\Delta_1}^0 + J_{\Delta_2}^0) m_o^3 + (4J_{\sim_1}^0 + J_{\sim_2}^0) m_e m_o^2 \\ & + 2(J_{\perp_1}^0 + J_{\perp_2}^0) m_e m_o^3 + J_{\diamond}^0 m_o^4 + J_{+}^0 m_e m_o^4 \end{aligned} \quad (4.32)$$

A similar expression for u_o can be obtained by simply exchanging in (4.32) the role of e and o.

4.2. The Mean Field equations

By using (4.25), (4.30), (4.31), and (4.32) we can finally write explicitly the free energy of the model in the Mean Field approximation. By minimizing such a free energy with respect to the magnetizations m_e and m_o , namely, by setting $\partial f / \partial m_e = \partial f / \partial m_o = 0$, with some algebra we get the two Mean Field equations

$$m_r = -\tanh \left[\beta \frac{\partial}{\partial m_r} (u_e + u_o) \right] \quad \text{with} \quad r = e, o \quad (4.33)$$

A straightforward computation gives the derivatives

$$\begin{aligned} -\frac{\partial u_e}{\partial m_e} = & J_{\bullet}^0 + 2(J_{\langle 1 \rangle}^0 + J_{\langle 2 \rangle}^0) m_o + (4J_{\sim_1}^0 + J_{\sim_2}^0) m_o^2 + 2(J_{\perp_1}^0 + J_{\perp_2}^0) m_o^3 \\ & + J_{+}^0 m_o^4 \\ -\frac{\partial u_e}{\partial m_o} = & 2(J_{o_1}^0 + J_{o_2}^0) + 2(J_{\langle 1 \rangle}^0 + J_{\langle 2 \rangle}^0) m_e + 2(4J_{\langle \rangle}^0 + J_{\langle \langle \rangle \rangle_1}^0 + J_{\langle \langle \rangle \rangle_2}^0) m_o \\ & + 6(J_{\Delta_1}^0 + J_{\Delta_2}^0) m_o^2 + 2(4J_{\sim_1}^0 + J_{\sim_2}^0) m_e m_o \\ & + 6(J_{\perp_1}^0 + J_{\perp_2}^0) m_e m_o^2 + 4J_{\diamond}^0 m_o^3 + 4J_{+}^0 m_e m_o^3 \end{aligned} \quad (4.34)$$

and

$$\begin{aligned} -\frac{\partial u_o}{\partial m_e} = & 2(J_{o_1}^0 + J_{o_2}^0) + 2(J_{\langle 1 \rangle}^0 + J_{\langle 2 \rangle}^0) m_o + 2(4J_{\langle \rangle}^0 + J_{\langle \langle \rangle \rangle_1}^0 + J_{\langle \langle \rangle \rangle_2}^0) m_e \\ & + 6(J_{\Delta_1}^0 + J_{\Delta_2}^0) m_e^2 + 2(4J_{\sim_1}^0 + J_{\sim_2}^0) m_o m_e \\ & + 6(J_{\perp_1}^0 + J_{\perp_2}^0) m_o m_e^2 + 4J_{\diamond}^0 m_e^3 + 4J_{+}^0 m_o m_e^3 \\ -\frac{\partial u_o}{\partial m_o} = & J_{\bullet}^0 + 2(J_{\langle 1 \rangle}^0 + J_{\langle 2 \rangle}^0) m_e + (4J_{\sim_1}^0 + J_{\sim_2}^0) m_e^2 + 2(J_{\perp_1}^0 + J_{\perp_2}^0) m_e^3 \\ & + J_{+}^0 m_e^4 \end{aligned} \quad (4.35)$$

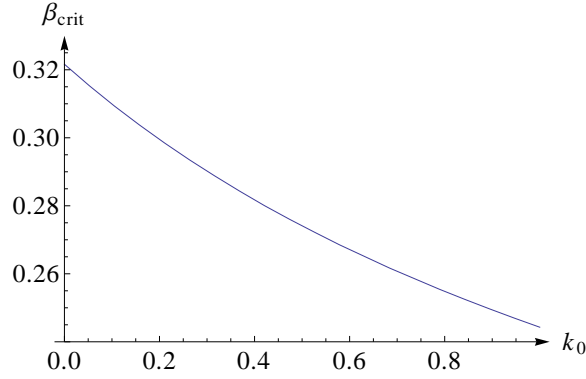


Figure 4.7: Critical temperature β_{crit} as function of k_0 at $h = 0$ and $k_1 = k_2 = 1$.

4.3. Mean Field results

We are interested to study the behavior of the critical transition between the paramagnetic and the ferromagnetic one at $h = 0$ and the structure of the low-temperature phase diagram.

As discussed in Subsection 3.3, at $k_0 = 0$ the model behaves as two decoupled standard Ising models so that it exhibits a second order phase transition at $\beta = \log(1 + \sqrt{2})/2 \approx 0.4407$ (the classical Onsager critical temperature). By studying in this region the Mean Field equation, we find a continuous transition at $\beta = 0.3216(5)$. In the case $k_1 = k_2 = 1$ and $k_0 = 1$, it was shown in [24, section 7.2.3] through Monte-Carlo simulations that $\beta_{\text{crit}} \approx 0.32$ to be compare with $\beta_{\text{crit}} \approx 0.24$ in the Mean Field approximation. These results are not surprising at all, indeed the Mean Field approximation always provides a larger estimate for the critical temperature.

What we are interested in is trying to understand the effect of the self-interaction on the behavior of the model. Hence, to understand if at $k_0 > 0$ the critical transition is still present and to estimate the value of the corresponding critical temperature.

By solving the Mean Field equation for $k_0 \in [0, 1]$, we always find a critical transition and the value of the critical inverse temperature $\beta_{\text{crit}}(k_0)$ decreases when k_0 is increased. Our results are depicted in figure 4.7.

As explained in the introduction, our main concern is that of understanding how the zero-temperature phase diagram, see figure 3.6, is modified at small positive temperatures. In view of the ground state structure we expect the presence of four phases: positive ferromagnetic, negative ferromagnetic, odd, and even checkerboard. The first two phases are respectively characterized by positive and negative magnetization, while the last two by a positive and negative staggered magnetization.

In the sequel we will not distinguish between the two checkerboard phases, since they

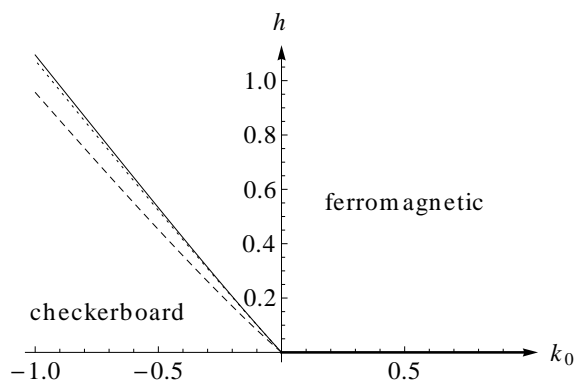


Figure 4.8: Phase diagram at different values of β in the plane k_0 - h with $k_1 = k_2 = 1$. In the region $k_0 < 0$ the three lines are the first order transition line between the positive ferromagnetic and the checkerboard phases. Continuous, dotted, and dashed lines refer, respectively, to the cases $\beta = 1.2, 0.8, 0.4$. In the region $k_0 > 0$ the horizontal $h = 0$ axis is the first order transition line between the two ferromagnetic phases. The phase diagram in the region $h < 0$ can be constructed by symmetry.

are equivalent. Moreover, we shall discuss the phase diagram only in the region $h > 0$. The case $h < 0$ can then be recovered by using the spin-flip symmetry.

For $h > 0$, in order to draw the Mean Field phase diagram we identify the two different phases (checkerboard) and positive ferromagnetic by solving iteratively the Mean Field equations (4.33) starting from a suitable initial point, namely, $m_e = m_o = 0.8$ for the ferromagnetic phase and $m_e = 0.8$ and $m_o = -0.8$ for the checkerboard one. We shall decide about the phase of the system by choosing the one with smallest Mean Field free energy. The free energy will be computed by using (4.25), (4.30), (4.31), and (4.32).

Mean Field predictions are summarized in figure 4.8, where the phase diagram of the cross PCA is plotted on the k_0 - h plane at different values of β . More precisely, we considered the values $\beta = 1.2, 0.8, 0.4$.

The most important remark is that the triple point is not affected by the temperature, indeed, its position is constantly the origin of the k_0 - h plane for each value of β . In other words the Mean Field approximation confirms the conjecture based on the entropy argument quoted in the introduction [8].

For the sake of completeness we briefly recall this argument. At finite temperature, ground states are perturbed because small droplets of different phases show up. The idea is to calculate the energetic cost of a perturbation of one of the four coexisting states via the formation of a square droplet of a different phase. If it results that one of the four ground

states is more easily perturbed, then we will conclude that this is the equilibrium phase at finite temperature.

The energy cost of a square droplet of side length ℓ of one of the two homogeneous ferromagnetic ground states plunged in one of the two checkerboards (or vice versa) is equal to 8ℓ . On the other hand if an homogeneous phase is perturbed as above by the other homogeneous phases, or one of the two checkerboards is perturbed by the other one, then the energy cost is 16ℓ . Hence, from the energetic point of view the most convenient excitations are those in which a homogeneous phase is perturbed by a checkerboard or vice versa. Moreover, for each state $\mathbf{d}, \mathbf{u}, \mathbf{c}_e, \mathbf{c}_o$ there exist two possible energetically convenient excitations: there is no entropic reason to prefer one of the four ground states to the others when a finite low-temperature is considered. This is why it is possible to conjecture that at small finite temperature the four ground states still coexist.

Finally we note that the Mean Field prediction for the ferro-checkerboard phase transition is that such a transition is discontinuous. And this result does not depend on the value of the temperature.

5. Conclusions

In this paper we have discussed some general properties of the Hamiltonian associated with a class of reversible Probabilistic Cellular Automata. We have focused our attention to the so-called cross PCA model, which is a two-dimensional reversible PCA in which the updating rule of a cell depends on the status of the five cells forming a cross centered at the cell itself.

This model had been extensively studied from the metastability point of view and many interesting properties have been shown. In particular a suggestive analogy with the Blume-Capel model had been pointed out in the metastability literature.

In this paper we focused our attention on the structure of the potentials describing the microscopic interaction and on the zero and positive small temperature phase diagram. We computed the zero-temperature phase diagram exactly with respect to the self-interaction intensity and the magnetic field.

At finite temperature the phase diagram has been derived in the framework of a suitable Mean Field approximation. We have discussed the variation of the critical temperature for the transition between the ordered and the disordered phase at zero magnetic field as a function of the self-interaction intensity. We have shown that, in the Mean Field approximation, such a temperature is an increasing function of the self-interaction intensity.

Moreover we have discussed the low-temperature phase diagram in the plane k_0-h and have shown that the topology of the zero temperature phase diagram is preserved when the temperature is positive and small. Finally, we have shown that the Mean Field approximation

is consistent with an entropic heuristic argument suggesting that the position of the zero-temperature triple point is not changed at low-temperature.

A. Coupling constants

In this appendix we report the expression of the coupling constants defined in Section 3.1 (see also figure 3.3) as function of h , β , k_0 , k_1 , and k_2 . The scheme we adopted for the computation is described in Section 3.1 as well. For the couplings in which we had to distinguish between the horizontal and the vertical case we report only the horizontal one and note that the corresponding vertical one can be obtained by exchanging in the formula the role of k_1 and k_2 .

$$J_{\bullet}^0 = \frac{1}{5}h + \frac{1}{2^5\beta} \log \left\{ \frac{\cosh^4[\beta(h+k_0)]}{\cosh^4[\beta(h-k_0)]} \times \frac{\cosh^2[\beta(h+k_0+2k_1)] \cosh^2[\beta(h+k_0-2k_1)]}{\cosh^2[\beta(h-k_0+2k_1)] \cosh^2[\beta(h-k_0-2k_1)]} \times \frac{\cosh^2[\beta(h+k_0+2k_2)] \cosh^2[\beta(h+k_0-2k_2)]}{\cosh^2[\beta(h-k_0+2k_2)] \cosh^2[\beta(h-k_0-2k_2)]} \times \frac{\cosh[\beta(h+k_0+2(k_1-k_2))] \cosh[\beta(h+k_0-2(k_1-k_2))]}{\cosh[\beta(h-k_0+2(k_1-k_2))] \cosh[\beta(h-k_0-2(k_1-k_2))]} \times \frac{\cosh[\beta(h+k_0+2(k_1+k_2))] \cosh[\beta(h+k_0-2(k_1+k_2))]}{\cosh[\beta(h-k_0+2(k_1+k_2))] \cosh[\beta(h-k_0-2(k_1+k_2))]} \right\} \quad (\text{A.36})$$

$$J_{o_1}^0 = \frac{1}{5}h + \frac{1}{2^5\beta} \log \left\{ \frac{\cosh^2[\beta(h-k_0+2k_1)] \cosh^2[\beta(h+k_0+2k_1)]}{\cosh^2[\beta(h-k_0-2k_1)] \cosh^2[\beta(h+k_0-2k_1)]} \times \frac{\cosh[\beta(h+k_0+2(k_1-k_2))] \cosh[\beta(h-k_0+2(k_1-k_2))]}{\cosh[\beta(h+k_0-2(k_1-k_2))] \cosh[\beta(h-k_0-2(k_1-k_2))]} \times \frac{\cosh[\beta(h+k_0+2(k_1+k_2))] \cosh[\beta(h-k_0+2(k_1+k_2))]}{\cosh[\beta(h+k_0-2(k_1+k_2))] \cosh[\beta(h-k_0-2(k_1+k_2))]} \right\} \quad (\text{A.37})$$

$$J_{\langle 1}^0 = \frac{1}{2^5\beta} \log \left\{ \frac{\cosh^2[\beta(h-k_0-2k_1)] \cosh^2[\beta(h+k_0+2k_1)]}{\cosh^2[\beta(h+k_0-2k_1)] \cosh^2[\beta(h-k_0+2k_1)]} \times \frac{\cosh[\beta(h+k_0+2k_1-2k_2)] \cosh[\beta(h-k_0-2k_1+2k_2)]}{\cosh[\beta(h-k_0+2k_1-2k_2)] \cosh[\beta(h+k_0-2k_1+2k_2)]} \times \frac{\cosh[\beta(h-k_0-2(k_1+k_2))] \cosh[\beta(h+k_0+2(k_1+k_2))]}{\cosh[\beta(h+k_0-2(k_1+k_2))] \cosh[\beta(h-k_0+2(k_1+k_2))]} \right\} \quad (\text{A.38})$$

$$J_{\langle\langle\rangle\rangle}^0 = \frac{1}{2^5\beta} \log \left\{ \frac{\cosh[\beta(h - k_0 - 2(k_1 + k_2))] \cosh[\beta(h + k_0 - 2(k_1 + k_2))]}{\cosh[\beta(h - k_0 + 2k_1 - 2k_2)] \cosh[\beta(h + k_0 + 2k_1 - 2k_2)]} \right. \\ \left. \times \frac{\cosh[\beta(h - k_0 + 2(k_1 + k_2))] \cosh[\beta(h + k_0 + 2(k_1 + k_2))]}{\cosh[\beta(h - k_0 - 2k_1 + 2k_2)] \cosh[\beta(h + k_0 - 2k_1 + 2k_2)]} \right\} \quad (\text{A.39})$$

$$J_{\langle\langle\langle\rangle\rangle\rangle_1}^0 = \frac{1}{2^5\beta} \log \left\{ \frac{\cosh^2[\beta(h - k_0 - 2k_1)] \cosh^2[\beta(h + k_0 - 2k_1)]}{\cosh^2[\beta(h - k_0 - 2k_2)] \cosh^2[\beta(h + k_0 - 2k_2)]} \right. \\ \times \frac{\cosh^2[\beta(h - k_0 + 2k_1)] \cosh^2[\beta(h + k_0 + 2k_1)]}{\cosh^2[\beta(h - k_0 + 2k_2)] \cosh^2[\beta(h + k_0 + 2k_2)]} \\ \times \frac{1}{\cosh^4[\beta(h + k_0)] \cosh^4[\beta(h - k_0)]} \\ \times \cosh[\beta(h - k_0 + 2(k_1 - k_2))] \cosh[\beta(h + k_0 + 2(k_1 - k_2))] \\ \times \cosh[\beta(h - k_0 - 2(k_1 - k_2))] \cosh[\beta(h + k_0 - 2(k_1 - k_2))] \\ \times \cosh[\beta(h - k_0 - 2(k_1 + k_2))] \cosh[\beta(h + k_0 - 2(k_1 + k_2))] \\ \left. \times \cosh[\beta(h - k_0 + 2(k_1 + k_2))] \cosh[\beta(h + k_0 + 2(k_1 + k_2))] \right\} \quad (\text{A.40})$$

$$J_{\Delta_1}^0 = \frac{1}{2^5\beta} \log \left\{ \frac{\cosh^2[\beta(h - k_0 - 2k_2)] \cosh^2[\beta(h + k_0 - 2k_2)]}{\cosh^2[\beta(h - k_0 + 2k_2)] \cosh^2[\beta(h + k_0 + 2k_2)]} \right. \\ \times \frac{\cosh[\beta(h - k_0 - 2k_1 + 2k_2)] \cosh[\beta(h + k_0 - 2k_1 + 2k_2)]}{\cosh[\beta(h - k_0 + 2k_1 - 2k_2)] \cosh[\beta(h + k_0 + 2k_1 - 2k_2)]} \\ \times \frac{\cosh[\beta(h - k_0 + 2(k_1 + k_2))] \cosh[\beta(h + k_0 + 2(k_1 + k_2))]}{\cosh[\beta(h - k_0 - 2(k_1 + k_2))] \cosh[\beta(h + k_0 - 2(k_1 + k_2))]} \left. \right\} \quad (\text{A.41})$$

$$J_{\sqcup}^0 = \frac{1}{2^5\beta} \log \left\{ \frac{\cosh[\beta(h - k_0 + 2(k_1 - k_2))] \cosh[\beta(h - k_0 - 2(k_1 - k_2))]}{\cosh[\beta(h + k_0 + 2(k_1 - k_2))] \cosh[\beta(h + k_0 - 2(k_1 - k_2))]} \right. \\ \times \frac{\cosh[\beta(h + k_0 - 2(k_1 + k_2))] \cosh[\beta(h + k_0 + 2(k_1 + k_2))]}{\cosh[\beta(h - k_0 - 2(k_1 + k_2))] \cosh[\beta(h - k_0 + 2(k_1 + k_2))]} \left. \right\} \quad (\text{A.42})$$

$$J_{\sim_1}^0 = \frac{1}{2^5 \beta} \log \left\{ \frac{\cosh^4[\beta(h - k_0)] \cosh^2[\beta(h + k_0 - 2k_1)] \cosh^2[\beta(h + k_0 + 2k_1)]}{\cosh^4[\beta(h + k_0)] \cosh^2[\beta(h - k_0 - 2k_1)] \cosh^2[\beta(h - k_0 + 2k_1)]} \right. \\
\times \frac{\cosh^2[\beta(h - k_0 - 2k_2)] \cosh^2[\beta(h - k_0 + 2k_2)]}{\cosh^2[\beta(h + k_0 - 2k_2)] \cosh^2[\beta(h + k_0 + 2k_2)]} \\
\times \frac{\cosh[\beta(h + k_0 + 2(k_1 - k_2))] \cosh[\beta(h + k_0 - 2(k_1 - k_2))]}{\cosh[\beta(h - k_0 + 2(k_1 - k_2))] \cosh[\beta(h - k_0 - 2(k_1 - k_2))]} \\
\left. \times \frac{\cosh[\beta(h + k_0 - 2(k_1 + k_2))] \cosh[\beta(h + k_0 + 2(k_1 + k_2))]}{\cosh[\beta(h - k_0 - 2(k_1 + k_2))] \cosh[\beta(h - k_0 + 2(k_1 + k_2))]} \right\} \quad (\text{A.43})$$

$$J_{\perp_1}^0 = \frac{1}{2^5 \beta} \log \left\{ \frac{\cosh^2[\beta(h + k_0 - 2k_2)] \cosh^2[\beta(h - k_0 + 2k_2)]}{\cosh^2[\beta(h - k_0 - 2k_2)] \cosh^2[\beta(h + k_0 + 2k_2)]} \right. \\
\times \frac{\cosh[\beta(h - k_0 + 2(k_1 - k_2))] \cosh[\beta(h + k_0 - 2(k_1 - k_2))]}{\cosh[\beta(h + k_0 + 2(k_1 - k_2))] \cosh[\beta(h - k_0 - 2(k_1 - k_2))]} \\
\left. \times \frac{\cosh[\beta(h - k_0 - 2(k_1 + k_2))] \cosh[\beta(h + k_0 + 2(k_1 + k_2))]}{\cosh[\beta(h + k_0 - 2(k_1 + k_2))] \cosh[\beta(h - k_0 + 2(k_1 + k_2))]} \right\} \quad (\text{A.44})$$

$$J_{\diamond}^0 = \frac{1}{2^5 \beta} \log \left\{ \cosh^4[\beta(h - k_0)] \cosh^4[\beta(h + k_0)] \right. \\
\times \frac{\cosh[\beta(h - k_0 - 2(k_1 + k_2))] \cosh[\beta(h + k_0 - 2(k_1 + k_2))]}{\cosh^2[\beta(h - k_0 - 2k_1)] \cosh^2[\beta(h + k_0 - 2k_1)]} \\
\times \frac{\cosh[\beta(h - k_0 + 2(k_1 + k_2))] \cosh[\beta(h + k_0 + 2(k_1 + k_2))]}{\cosh^2[\beta(h - k_0 + 2k_1)] \cosh^2[\beta(h + k_0 + 2k_1)]} \\
\times \frac{\cosh[\beta(h - k_0 + 2(k_1 - k_2))] \cosh[\beta(h + k_0 + 2(k_1 - k_2))]}{\cosh^2[\beta(h - k_0 - 2k_2)] \cosh^2[\beta(h + k_0 - 2k_2)]} \\
\left. \times \frac{\cosh[\beta(h - k_0 - 2(k_1 - k_2))] \cosh[\beta(h + k_0 - 2(k_1 - k_2))]}{\cosh^2[\beta(h - k_0 + 2k_2)] \cosh^2[\beta(h + k_0 + 2k_2)]} \right\} \quad (\text{A.45})$$

$$J_{+}^0 = \frac{1}{2^5 \beta} \log \left\{ \frac{\cosh^4[\beta(h + k_0)] \cosh^2[\beta(h - k_0 - 2k_1)] \cosh^2[\beta(h - k_0 + 2k_1)]}{\cosh^4[\beta(h - k_0)] \cosh^2[\beta(h + k_0 - 2k_1)] \cosh^2[\beta(h + k_0 + 2k_1)]} \right. \\
\times \frac{\cosh^2[\beta(h - k_0 - 2k_2)] \cosh^2[\beta(h - k_0 + 2k_2)]}{\cosh^2[\beta(h + k_0 - 2k_2)] \cosh^2[\beta(h + k_0 + 2k_2)]} \\
\times \frac{\cosh[\beta(h + k_0 + 2(k_1 - k_2))] \cosh[\beta(h + k_0 - 2(k_1 - k_2))]}{\cosh[\beta(h - k_0 + 2(k_1 - k_2))] \cosh[\beta(h - k_0 - 2(k_1 - k_2))]} \\
\left. \times \frac{\cosh[\beta(h + k_0 - 2(k_1 + k_2))] \cosh[\beta(h + k_0 + 2(k_1 + k_2))]}{\cosh[\beta(h - k_0 - 2(k_1 + k_2))] \cosh[\beta(h - k_0 + 2(k_1 + k_2))]} \right\} \quad (\text{A.46})$$

Acknowledgments. The authors thank J. Bricmont, A. Pelizzola, and A. van Enter for some very useful discussions, comments, and references. P.-Y. Louis thanks EURANDOM/TU Eindhoven, Utrecht University, and Dipartimento SBAI (Sapienza Università di Roma) where part of this work was done and the CNRS for supporting these research stays. E.N.M. Cirillo thanks Technical University Delft, Utrecht Mathematics Department and EURANDOM/TU Eindhoven for their kind hospitality and financial support.

References

- [1] S. Bigelis, E.N.M. Cirillo, J.L. Lebowitz, E.R. Speer, “Critical droplets in metastable probabilistic cellular automata,” *Phys. Rev. E* **59**, 3935, (1999).
- [2] M. Blume, “Theory of the First-Order Magnetic Phase Change in UO_2 ,” *Phys. Rev.* **141**, 517, (1966).
- [3] M. Blume, V.J. Emery, R.B. Griffiths, “Ising Model for the λ Transition and Phase Separation in He^3 – He^4 Mixtures,” *Phys. Rev. A* **4**, 1071–1077, (1971).
- [4] J. Bricmont, J. Slawny, “Phase Transitions in Systems with a Finite Number of Dominant Ground States,” *Journ. Stat. Phys.* **54**, 89, (1989).
- [5] H.W. Capel, “On possibility of first-order phase transitions in Ising systems of triplet ions with zero-field splitting,” *Physica* **32**, 966, (1966).
- [6] A. Capi, P. Colangelo, G. Gonnella, A. Maritan, “Ensemble of interacting random surfaces on a lattice,” *Nuclear Physics B* **370**, 659–694, (1992).
- [7] E.N.M. Cirillo, F.R. Nardi, C. Spitoni, “Metastability for a reversible probabilistic cellular automata with self-interaction,” *Journ. Stat. Phys.* **132**, 431–471, (2008).
- [8] E.N.M. Cirillo, F.R. Nardi, “Metastability for the Ising model with a parallel dynamics,” *Journ. Stat. Phys.* **110**, 183–217, (2003).
- [9] E.N.M. Cirillo, F.R. Nardi, C. Spitoni, “Competitive nucleation in reversible Probabilistic Cellular Automata,” *Physical Review E* **78**, 040601, (2008).
- [10] E.N.M. Cirillo, F.R. Nardi, C. Spitoni, “Competitive nucleation in metastable systems.” *Applied and Industrial Mathematics in Italy III. Series on Advances in Mathematics for Applied Sciences*, Volume **82**, 208–219, (2010).

- [11] E.N.M. Cirillo, F.R. Nardi, A.D. Polosa, “Magnetic order in the Ising model with parallel dynamics.” *Phys. Rev. E* **64**, 57103, (2001).
- [12] E.N.M. Cirillo, E. Olivieri, “Metastability and nucleation for the Blume-Capel model. Different mechanisms of transition,” *Journ. Stat. Phys.* **83**, 473–554, (1996).
- [13] E.N.M. Cirillo, S. Stramaglia, “Polymerization in a ferromagnetic spin model with threshold.” *Phys. Rev. E* **54**, 1096, (1996).
- [14] P. Dai Pra, P.-Y. Louis, S. Roelly, “Stationary measures and phase transition for a class of probabilistic cellular automata.” *ESAIM Probab. Statist.* **6**, 89–104, (2002).
- [15] B. Derrida, “Dynamical phase transition in spin model and automata,” Fundamental problem in Statistical Mechanics VII, H. van Beijeren, Editor, Elsevier Science, (1990).
- [16] A. Georges and P. Le Doussal, “From equilibrium spin models to probabilistic cellular automata”, *Journal of Statistical Physics*, **54**, 3-4, 1011–1064, (1989).
- [17] Goldstein S., Kuik R., Lebowitz J.L., Maes C., “From PCAs to equilibrium systems and back”, *Comm. Math. Phys.*, **125**, no. 1, 71–79, (1989).
- [18] G. Grinstein, C. Jayaprakash, and Y. He, “Statistical Mechanics of Probabilistic Cellular Automata” *Phys. Rev. Lett.* **55**, 2527, (1985).
- [19] K. Haller, T. Kennedy, “Absence of renormalization group pathologies near the critical temperature. Two examples.” *Journ. Stat. Phys.* **85**, 607–637, (1996).
- [20] J. Kari, “Theory of cellular automata: A survey”, *Theoretical Computer Science*, Volume **334**, Issues 1-3, 3–33, (2005).
- [21] V. Kozlov, N.B. Vasiljev, “Reversible Markov chain with local interactions,” in “Multi-component random system,” 451–469, Adv. in Prob. and Rel. Topics, (1980).
- [22] L. Lam, “Non-Linear Physics for Beginners: Fractals, Chaos, Pattern Formation, Solitons, Cellular Automata and Complex Systems”, book, World Scientific, (1998).
- [23] Lebowitz J.L., Maes C., Speer E.R., “Statistical mechanics of probabilistic cellular automata.”, *J. Statist. Phys.* **59**, 1-2, 117–170, (1990).
- [24] P.-Y. Louis. “Automates Cellulaires Probabilistes : mesures stationnaires, mesures de Gibbs associées et ergodicité”, *PhD thesis*, Université Lille I and Politecnico di Milano, sept. 2002. http://tel.archives-ouvertes.fr/index.php?halsid=2amredt6j0va4869evh5q209e3&view_this_doc=tel-00002203&version=2

- [25] P.-Y. Louis. “Ergodicity of PCA: equivalence between spatial and temporal mixing conditions”, *Electronic Communications in Probability*, **9**, 119–131, (2004).
- [26] P.-Y. Louis and J.-B. Rouquier. “Time-to-coalescence for interacting particle systems: Parallel versus sequential updating.”, *Preprint 2009/03*, Universität Potsdam, ISSN no. 1613-3307 (2009)
<http://nbn-resolving.de/urn:nbn:de:kobv:517-opus-49454>.
- [27] F.R. Nardi, C. Spitoni, “Sharp asymptotics for stochastic dynamics with parallel updating rule.” *Journal of Statistical Physics*, **146**, 701–718, (2012).
- [28] J. Palandi, R.M.C. de Almeida, J.R. Iglesias, M. Kiwi, “Cellular automaton for the order-disorder transition”, *Chaos, Solitons & Fractals*, Vol. **6**, 439–445, (1995).
- [29] M. Perc, J. Gómez-Gardeñes, A. Szolnoki, L.M. Floría, and Y. Moreno, “Evolutionary dynamics of group interactions on structured populations: A review”, *J. R. Soc. Interface* **10**, 20120997, (2013).
- [30] M. Perc and P. Grigolini, “Collective behavior and evolutionary games – An introduction”, *Chaos, Solitons & Fractals* **56**, 1–5, (2013).
- [31] M. Perc and A. Szolnoki, “Coevolutionary games – A mini review”, *Biosystems* **99**, 109–125, (2010).
- [32] G.Ch. Sirakoulis and S. Bandini (editors), “Cellular Automata: 10th International Conference on Cellular Automata for Research and Industry”, ACRI 2012, *Proceedings, 2012, Lecture Notes in Computer Science*, Springer (2012).
- [33] J. Slawny, “Low-Temperature Properties of Classical Lattice Systems: Phase Transitions and Phase Diagrams”, in *Phase Transitions and Critical Phenomena*, vol. **11**, C. Domb and J.L. Lebowitz, eds. Academic Press, London, (1987).
- [34] A.L. Toom , N.B. Vasilyev, O.N. Stavskaya, L.G. Mityushin, G.L. Kurdyumov, S.A. Pirogov, *Discrete local Markov systems*, in *Stochastic Cellular Systems: ergodicity, memory, morphogenesis*, edited by R.L. Dobrushin, V.I. Kryukov, A.L. Toom, Manchester University Press, 1–182, (1990).
- [35] L.N. Vasershtein, ”Markov processes over denumerable products of spaces describing large system of automata”, *Problemy Peredači Informacii* **5**, no. 3, 64–72, (1969).
- [36] S. Wolfram, “Statistical mechanics of cellular automata”, *Rev. Mod. Phys.*, **55**, 3, 601–644, (1983).

- [37] S. Wolfram, "Universality and complexity in cellular automata", *Physica D: Nonlinear Phenomena*, Vol. **10**, Issues 1-2, 1–35, (1984).
- [38] S. Wolfram, "Cellular automata as models of complexity", *Nature* **311**, 419–424, (1984).